Modern radio engineering and telecommunication systems

Современные радиотехнические и телекоммуникационные системы

UDC 621.391.072
https://doi.org/10.32362/2500-316X-2024-12-5-17-32
EDN EBOWFT

RESEARCH ARTICLE

Noise immunity of QAM-OFDM signal reception using soft-decision demodulation in the presence of narrowband interference

Alexey A. Paramonov @**,**
Chu Van Vuong

MIREA – Russian Technological University, Moscow, 194454 Russia
@ *Corresponding author, e-mail: paramonov@mirea.ru*

Abstract

Objectives. The aim of this paper is to study the noise immunity of digital information transmission in systems with orthogonal frequency division multiplexing (OFDM) and quadrature amplitude modulation (QAM) of subcarriers in the presence of narrowband interference. As a way of managing this interference, the paper studies the use of a demodulator with soft outputs and subsequent decoding of the convolutional code and low-density parity-check (LDPC) code used in the system.

Methods. The results presented in the article were obtained using statistical radio engineering, mathematical statistics, encoding theory, and computer modeling.

Results. The paper presents a simple method for calculating soft bit estimates in the *M*-point signal QAM demodulator, where *M* is an even power of two. A considerable amount of numerical results were obtained which show the dependence of the transmitted information bit error rate on *M*, as well as on the signal-to-noise ratio, signal-to-narrowband interference, and code rates.

Conclusions. It can be concluded from the above results that the use of encoding with soft demodulator decisions significantly improves the noise immunity of OFDM signal reception, and enables narrowband interference to be managed efficiently. LDPC encoding is superior to convolutional encoding in increasing the noise immunity of OFDM signal reception both in the absence and in the presence of narrowband interference. Along with the use in QAM-OFDM systems, the proposed simple method for demodulating QAM signals with soft decisions can be used in any wireless communication system using *M*-position QAM signals, where *M* is 2 to an even power.

Keywords: OFDM, soft decision, encoding, narrowband interference, noise immunity, bit error rate

• **Submitted:** 23.04.2024 • **Revised:** 19.06.2024 • **Accepted:** 05.08.2024

For citation: Paramonov A.A., Chu V.V. Noise immunity of QAM-OFDM signal reception using soft-decision demodulation in the presence of narrowband interference. *Russ. Technol. J.* 2024;12(5):17–32. https://doi.org/10.32362/2500-316X-2024-12-5-17-32

Financial disclosure: The authors have no financial or property interest in any material or method mentioned.

The authors declare no conflicts of interest.

НАУЧНАЯ СТАТЬЯ

Помехоустойчивость приема сигнала OFDM с использованием квадратурной амплитудной модуляции с мягкими решениями при наличии узкополосных помех

А.А. Парамонов [@], **В.В. Чу**

МИРЭА – Российский технологический университет, Москва, 119454 Россия
[@] *Автор для переписки, e-mail: paramonov@mirea.ru*

Резюме

Цели. Целью работы является исследование помехоустойчивости передачи цифровой информации в системах на основе мультиплексирования с ортогональным частотным разделением (orthogonal frequency division multiplexing, OFDM) и квадратурной амплитудной модуляцией (quadrature amplitude modulation, QAM) поднесущих в присутствии узкополосной помехи. В качестве способа борьбы с этой помехой исследовано применение демодулятора с мягкими выходами и последующее декодирование используемых в системе сверточного кода и кода LDPC (low-density parity-check code).

Методы. Представленные в статье результаты получены с использованием методов статистической радиотехники, математической статистики, теории кодирования и компьютерного моделирования.

Результаты. Представлен простой метод вычисления мягких оценок битов в демодуляторе *M*-ичных сигналов QAM, где *M* является четной степенью двойки. Получен большой объем численных результатов, показывающих зависимость вероятности ошибки на бит передаваемой информации от кратности *M*, от отношений сигнал/шум, сигнал/узкополосная помеха, от скорости кодов.

Выводы. Из полученных результатов можно сделать вывод, что использование кодирования с мягкими решениями демодулятора значительно улучшает помехоустойчивость приема OFDM-сигнала, позволяя эффективно бороться с узкополосными помехами. Кодирование LDPC показывает превосходство над сверточным кодированием в повышении помехоустойчивости приема сигнала OFDM как в отсутствие узкополосных помех, так и при их наличии. Наряду с использованием в системах QAM-OFDM, предложенный простой метод демодуляции сигналов QAM с мягкими решениями может применяться в любых системах беспроводной связи, использующих *M*-позиционные сигналы QAM, у которых *M* представляет собой число 2 в четной степени.

Ключевые слова: OFDM, квадратурная амплитудная модуляция, мягкое решение, кодирование, узкополосная помеха, помехоустойчивость, коэффициент битовых ошибок

• **Поступила:** 23.04.2024 • **Доработана:** 19.06.2024 • **Принята к опубликованию:** 05.08.2024

Для цитирования: Парамонов А.А., Чу В.В. Помехоустойчивость приема сигнала OFDM с использованием квадратурной амплитудной модуляции с мягкими решениями при наличии узкополосных помех. *Russ. Technol. J.* 2024;12(5):17–32. https://doi.org/10.32362/2500-316X-2024-12-5-17-32

Прозрачность финансовой деятельности: Авторы не имеют финансовой заинтересованности в представленных материалах или методах.

Авторы заявляют об отсутствии конфликта интересов.

INTRODUCTION

In modern wireless communication networks where the radio spectrum efficiency is crucial, data transmission systems based on orthogonal frequency division multiplexing (OFDM) [1–3] and quadrature amplitude modulation of M multiplicity (M-QAM) [4–6] are widely used. However, under conditions of the active use of spectrum and the presence of numerous sources of interference including narrowband ones [7, 8], reliable data transmission is becoming an urgent issue.

The aim of the paper is to investigate the noise immunity of the QAM-OFDM system with encoding in the presence of narrowband interference [9–11]. Decoding methods using demodulator hard decisions cannot often compensate for the impact of narrowband interference effectively, thus significantly degrading the reception quality. In this context, the method of soft demodulator decisions is proposed. This demodulator can be used effectively in conjunction with an appropriate decoder for improving reception noise immunity. The proposed soft decision algorithm for demodulation has a lower computational complexity when compared to conventional methods. The proposed method is based on analyzing the quality of the received signal, which allows the reliability degree to be determined dynamically for each bit of the transmitted signal. Thus, greater efficiency of the decoding process may be achieved, which results in increased noise immunity of the system in the presence of narrowband interference.

This paper describes the proposed method of demodulation of M-QAM signals with soft decisions, compared with existing demodulation methods, and simulation results showing its efficiency. It shows that the use of decoding with soft decisions allows for a noticeable improvement in noise immunity reception in the presence of narrowband interference.

OFDM SYSTEM AND SOFT DECISION ALGORITHM

The OFDM system considered in the paper is shown in Fig. 1.

Figure 1a shows the structure of the OFDM transmitter. The bit stream is encoded before modulation. The system is assumed to use M-QAM. After the inverse fast Fourier transform (IFFT), a guard interval is added to the OFDM signal, in order to protect the received signal from intersymbol interference. The signal is then transmitted over the air.

Figure 1b shows the structure of the OFDM receiver. In the receiver, signal processing is carried out in the reverse order to the transmitter processing order. Firstly, time synchronization and division of the OFDM signal into OFDM symbols are performed. After removing the guard interval, the fast Fourier transform (FFT) is performed. Then the signal is demodulated and finally decoded to obtain the original data stream.

The M-QAM signal $x(t)$ with symbol duration equal to the OFDM signal symbol duration is transmitted on each orthogonal frequency of the OFDM signal. Signal $\tilde{x}(t)$ received by the receiver on this frequency can be described as follows:

$$\tilde{x}(t) = x(t) + w(t), \quad (1)$$

wherein $w(t)$ stands for additive white Gaussian noise.

In such a problem statement, it would be reasonable to develop the algorithm for receiving the M-QAM signal. Including any additive interference into the received signal $\tilde{x}(t)$, except for noise, implies the information transmission system should necessarily operate on frequencies occupied by interference. A more realistic scenario is when the transmission system is designed to operate on frequencies free of interference. However, interference may actually occur, so the transmission system immunity should be analyzed separately for this case. It is thus from the positions referred to below, that the study of noise immunity to reception of QAM-OFDM signal in the presence of narrowband interference is carried out.

Here, it is worth noting the particular impact of harmonic interference on OFDM signal. The following formulas relating to harmonic interference assume that OFDM signal is shifted to zero frequency. Figure 1 shows that the received oscillation $\tilde{x}(t)$ is subjected to FFT procedure performed digitally. If this oscillation contains harmonic interference in the region of some subcarrier, it can be written as a sequence of time samples in the following way:

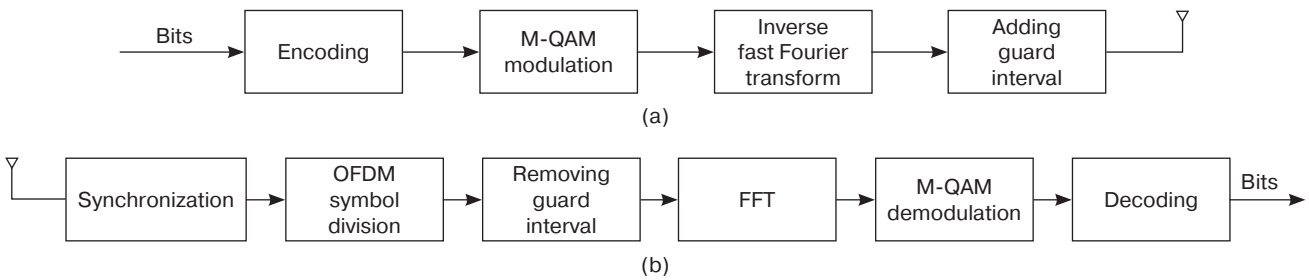

Fig. 1. The OFDM system structure: (a) transmitter, (b) receiver

$$g(n) = A_g e^{j(2\pi f_g n T_s + \theta)},$$

wherein A_g is the narrowband interference amplitude; f_g is the narrowband interference frequency; T_s is sampling interval equal to the symbol duration; and θ is the randomly distributed phase, $\theta \in (-\pi; \pi]$.

The narrowband interference frequency does not necessarily coincide with the subcarrier and is defined as follows:

$$f_g = \frac{m+\alpha}{N} f_s,\ 0 \le m \le N-1,\ -0.5 \le \alpha \le 0.5,$$

wherein f_s is frequency spacing between subcarriers; m is the number of the subcarrier closest to the interference; and N is the number of subcarriers in OFDM signal (and FFT dimensionality at reception).

Substituting f_g into the formula for harmonic interference and using the fact that $f_s = \frac{1}{T_s}$, the following can be obtained:

$$g(n) = A_g e^{j\left(\frac{2\pi}{N}(m+\alpha)n + \theta\right)}.$$

At $\alpha = 0$, the interference frequency coincides with the subcarrier frequency and the interference is orthogonal to other subcarriers. At $\alpha \neq 0$, the interference frequency does not coincide with the subcarrier frequency and this interference is not orthogonal to other subcarriers.

The expression for the narrowband interference spectrum after FFT is written as follows:

$$G(k) = \frac{1}{N}\sum_{n=0}^{N-1} g(n) e^{-\frac{j2\pi nk}{N}} = \frac{A_g}{N} e^{j\theta} \frac{1 - e^{j2\pi\alpha}}{1 - e^{j\frac{2\pi}{N}(m-k+\alpha)}}.$$

When the narrowband interference is orthogonal ($\alpha = 0$), it has the following form after FFT:

$$G(k) = \begin{cases} A_g e^{j\theta}, k = m, \\ 0, \quad k \neq m. \end{cases}$$

Thus, the narrowband interference coinciding in frequency with some mth subcarrier does not fall on frequencies of other subcarriers. If $\alpha \neq 0$, i.e., the narrowband interference is not orthogonal to other subcarriers, then the power of this interference is distributed over all subcarriers, i.e., a leakage of the interference spectrum occurs. The power of the narrowband interference leaked on some kth subcarrier due to non-orthogonality is determined by the following expression [7]:

$$\sigma^2_{G,k} = E[|G_k|^2] = \frac{A_g^2}{N^2} \cdot \frac{1 - \cos(2\pi\alpha)}{1 - \cos\frac{2\pi}{N}(m-k+\alpha)}.$$

Looking back to relation (1), its components can be represented as signal points in some signal space:

$$\tilde{X} = X + W. \tag{2}$$

The conditional probability density of the received signal $\tilde{X}$, given signal X, is transmitted can be written as follows:

$$f(\tilde{X} \mid X) = \frac{1}{\sqrt{2\pi\sigma^2}} e^{\left(-\frac{|\tilde{X}-X|^2}{2\sigma^2}\right)}. \tag{3}$$

Here, σ^2 is the distribution variance (3).

Each M-QAM signal symbols carries $\log_2 M$ bits of information. For example, for 16-QAM, the bits are b_0, b_1, b_2, and b_3. The soft decision for some ith bit is considered to be the logarithm of the likelihood ratio defined for a priori equal probability bits as follows [12–18]:

$$\begin{aligned} l(b_i) &= \ln \frac{\sum_{X \in S_i^-} f(X \mid \tilde{X})}{\sum_{X \in S_i^+} f(X \mid \tilde{X})} \approx \\ &\approx \ln \frac{\frac{1}{\sqrt{2\pi\sigma^2}} e^{\left(-\frac{|\tilde{X}-X_{i,\text{opt}}^-|^2}{2\sigma^2}\right)}}{\frac{1}{\sqrt{2\pi\sigma^2}} e^{\left(-\frac{|\tilde{X}-X_{i,\text{opt}}^+|^2}{2\sigma^2}\right)}} = \\ &= \frac{1}{2\sigma^2}(|\tilde{X} - X_{i,\text{opt}}^-|^2 - |\tilde{X} - X_{i,\text{opt}}^+|^2), \end{aligned} \tag{4}$$

where S_i^+ and S_i^- stand for sets of symbols whose ith bit is 1 and 0, respectively.

In expression (4), $X_{i,\text{opt}}^+$ and $X_{i,\text{opt}}^-$ are signals X closest to the received oscillation $\tilde{X}$ whose ith bit is 1 and 0, respectively:

$$\begin{aligned} X_{i,\text{opt}}^+ &= \arg\min_{X \in S_i^+} |\tilde{X} - X|^2, \\ X_{i,\text{opt}}^- &= \arg\min_{X \in S_i^-} |\tilde{X} - X|^2. \end{aligned} \tag{5}$$

Determining soft decisions by using expressions (4) and (5) is a rather cumbersome task. The complexity of calculations increases significantly with increasing

modulation level M. The next section examines considerably simpler algorithms for determining soft decisions for signals QAM with M being 2 in even power. The algorithms for 16-QAM, 64-QAM, and 256-QAM are set out in more detail.

SIMPLE ALGORITHMS FOR SOFT DECISION-MAKING IN M-QAM DEMODULATION

Figure 2 shows constellations for, 64-QAM, and 256-QAM. A decimal number is located near each signal point, and when converted into binary form it shows the set of transmitted binary symbols (hereinafter referred to as bits) corresponding to this signal point. For example, for 16-QAM signal, the point marked by number 6 corresponds to the set of transmitted bits: 0, 1, 1, 0.

We first examine the demodulation of 16-QAM signal. Each point of the signal constellation corresponds to 4 transmitted bits: b_0, b_1, b_2, and b_3. The projections of signal points on the in-phase and quadrature axes for different combinations of transmitted bits are shown in Table 1.

Figure 3 explains the proposed simplified algorithm for computing the logarithm of the likelihood ratio. Let a given symbol of 16-QAM signal be taken, as shown by a blue circle on the IQ-diagram: $\tilde{X}_i = \Re(\tilde{X}_i) + j\Im(\tilde{X}_i)$, where $\Re(\tilde{X}_i)$, $\Im(\tilde{X}_i)$ are real and imaginary parts of oscillation $\tilde{X}$.

The projections of signal points of the transmitted 16-QAM signal on axes I and Q are marked with red circles.

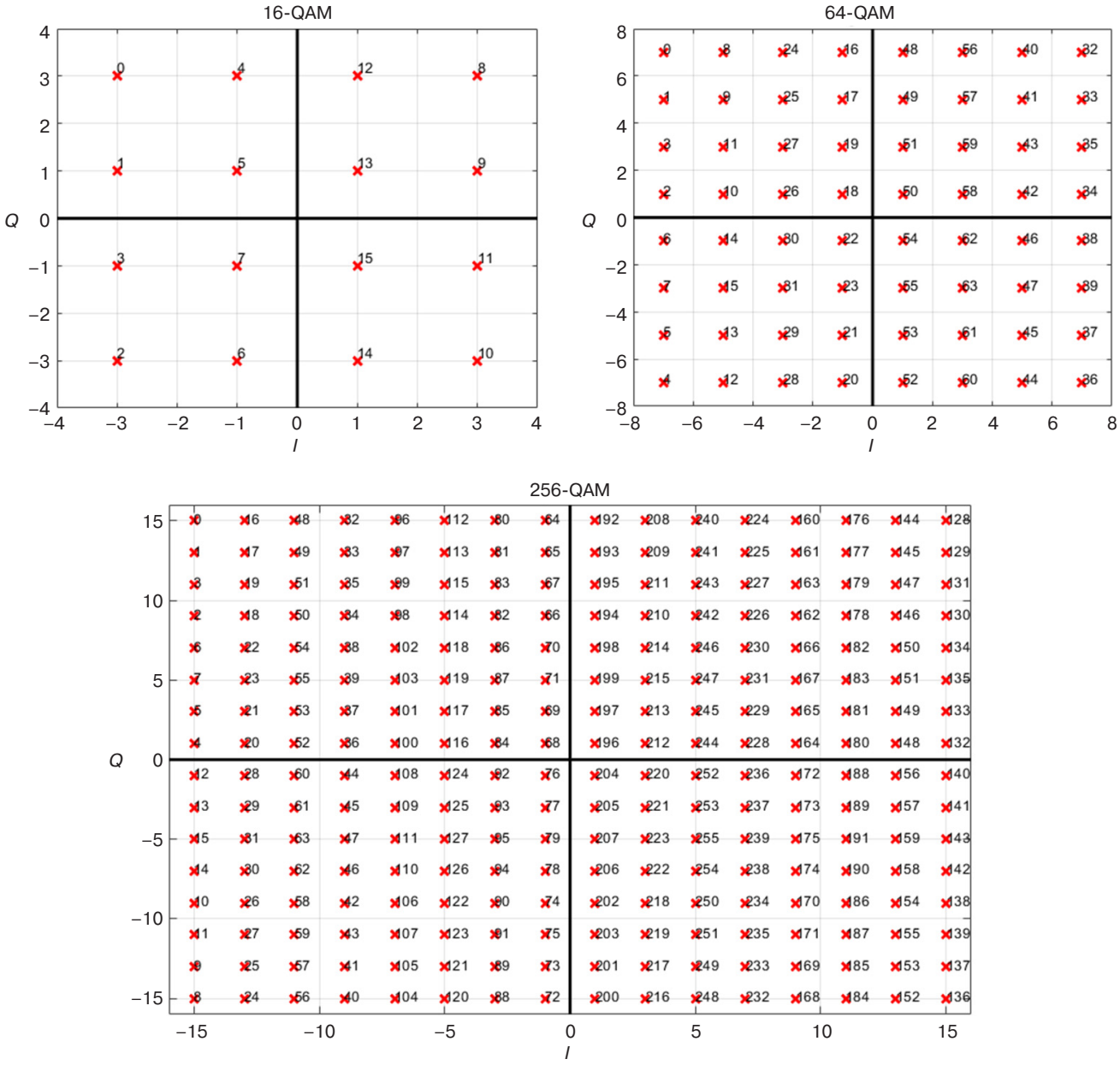

Fig. 2. M-QAM constellations

Table 1. Projections of signal points of 16-QAM signal on the *I* and *Q* axes

b_0b_1	I	b_2b_3	Q
00	−3	00	3
01	−1	01	1
11	+1	11	−1
10	+3	10	−3

It should be noted that the value of bit b_0 affects the projection of the signal point on the *I*-axis only, but does not affect the projection on the *Q*-axis. This can be clearly seen in Fig. 3a. When $b_0 = 0$, the real part of 16-QAM signal takes value −1 or −3. When $b_0 = 1$, the real part of the signal is +1 or +3.

The soft decision-making process for the first bit b_0 is shown in Fig. 4, representing the lower part of Fig. 3a.

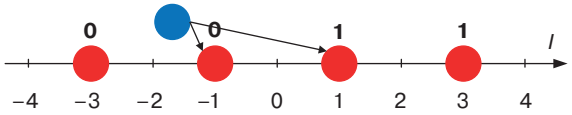

Fig. 4. Calculating the logarithm of the likelihood ratio for the 1st bit

The conditional probability of the received oscillation $\tilde{X}_i$ at $b_0 = 0$ is as follows:

$$P(\tilde{X}_i \mid b_0 = 0) = \frac{1}{\sqrt{2\pi\sigma^2}} e^{-\frac{(\Re(\tilde{X}_i)+3)^2}{2\sigma^2}} + \frac{1}{\sqrt{2\pi\sigma^2}} e^{-\frac{(\Re(\tilde{X}_i)+1)^2}{2\sigma^2}}. \quad (6)$$

The conditional probability of the received oscillation $\tilde{X}_i$ at $b_0 = 1$ is as follows:

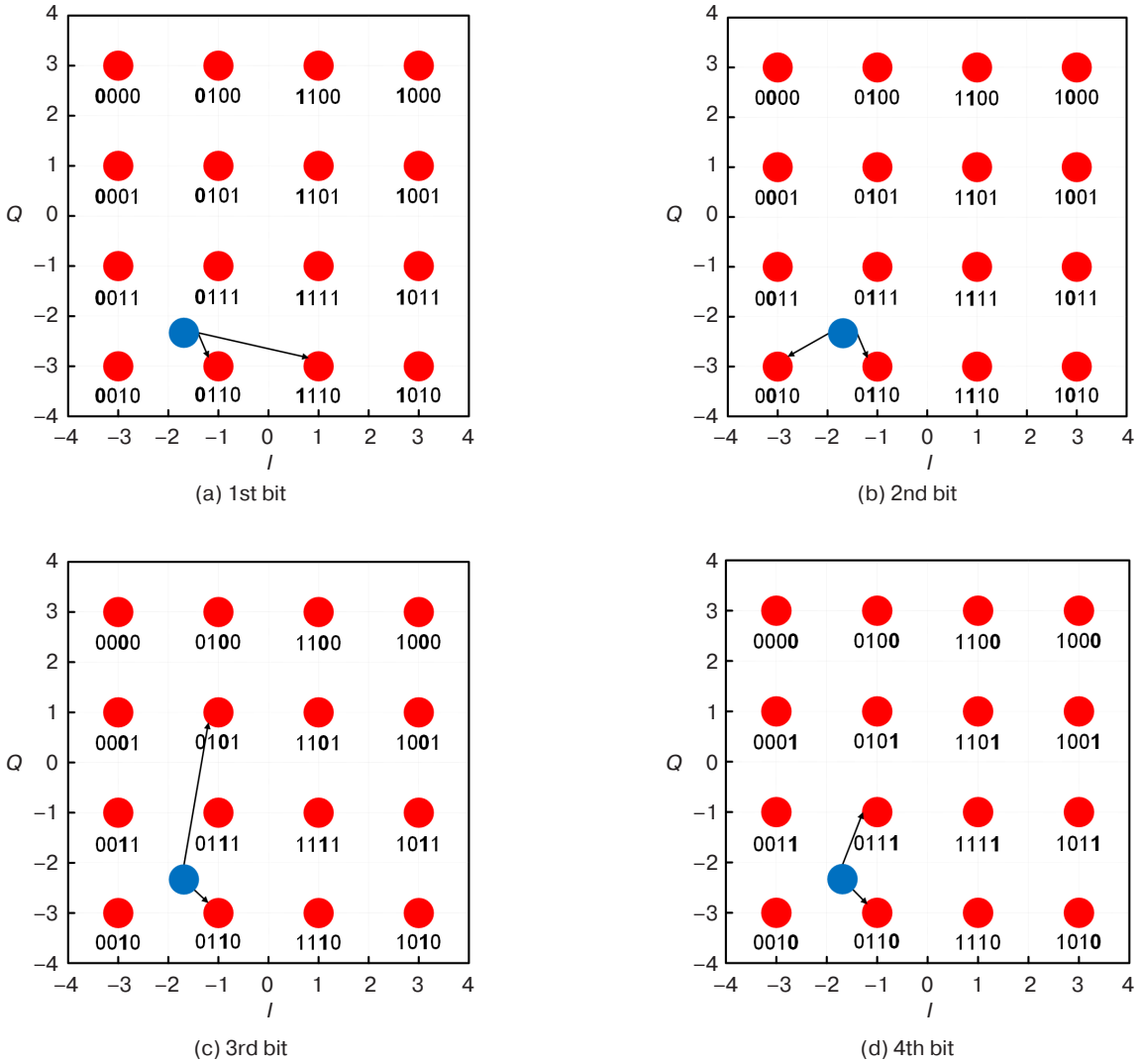

(a) 1st bit

(b) 2nd bit

(c) 3rd bit

(d) 4th bit

Fig. 3. Example of calculating the logarithms of likelihood ratios for each bit of 16-QAM signal

$$P(\tilde{X}_i \mid b_0 = 1) = \frac{1}{\sqrt{2\pi\sigma^2}} e^{-\frac{(\Re(\tilde{X}_i)-3)^2}{2\sigma^2}} + \frac{1}{\sqrt{2\pi\sigma^2}} e^{-\frac{(\Re(\tilde{X}_i)-1)^2}{2\sigma^2}}. \quad (7)$$

The likelihood ratio is described by the following expression:

$$\frac{P(\tilde{X}_i \mid b_0 = 0)}{P(\tilde{X}_i \mid b_0 = 1)} = \frac{e^{-\frac{(\Re(\tilde{X}_i)+1)^2}{2\sigma^2}} + e^{-\frac{(\Re(\tilde{X}_i)+3)^2}{2\sigma^2}}}{e^{-\frac{(\Re(\tilde{X}_i)-1)^2}{2\sigma^2}} + e^{-\frac{(\Re(\tilde{X}_i)-3)^2}{2\sigma^2}}}. \quad (8)$$

Using expression (8) is inconvenient since it requires that exponents be calculated. However, it can be simplified considering that the projection of the received oscillation in practice usually appears closer to one of the two possible signal points corresponding to a certain decision. For example, the projection of the received oscillation shown in Fig. 4 is closer to the value −1, rather than to −3, on which basis the decision on symbol $b_0 = 0$ is made. Given that expression (8) includes exponents of the squares of projection differences, it may be assumed that the first summand in denominator (8) is significantly larger than the second. Thus, the second exponent can be neglected. Similar reasoning is valid for evaluating numerator (8). Consequently, the logarithm of the likelihood ratio at value $\tilde{X}$ represented by the blue circle can be calculated quite accurately using the following expression:

$$l(b_0, \tilde{X}_i) \approx \frac{1}{2\sigma^2}((\Re(\tilde{X}_i)-1)^2 - (\Re(\tilde{X}_i)+1)^2) = -\frac{2}{\sigma^2}\Re(\tilde{X}_i). \quad (9)$$

When making the decision on bit b_1, reference should be made to Fig. 3b. The lower part of this figure is shown in Fig. 5. As in the previous case, the value of bit b_0 affects the projection of the signal point on the *I*-axis only and does not affect the projection on the *Q*-axis. At $b_1 = 0$, the real part of 16-QAM signal takes –3. When $b_1 = 1$, the real part of the signal takes –1, as shown in Fig. 5.

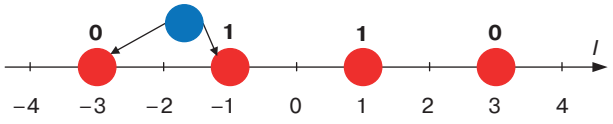

Fig. 5. Calculating the logarithm of the likelihood ratio for the 2nd bit

The likelihood ratio for the second bit b_1 of the received oscillation $\tilde{X}$ is the following:

$$l(b_1, \tilde{X}_i) \approx \frac{1}{2\sigma^2}((\Re(\tilde{X}_i)+1)^2 - (\Re(\tilde{X}_i)+3)^2) = -\frac{2}{\sigma^2}(\Re(\tilde{X}_i)+2). \quad (10)$$

For 16-QAM signals, only the projection of the signal point on the *Q*-axis varies depending on the value of bit b_2 (Fig. 3c). When $b_2 = 0$, the imaginary part of 16-QAM signal takes 1. When $b_2 = 1$, the imaginary part of the signal takes −3, as shown in Fig. 6.

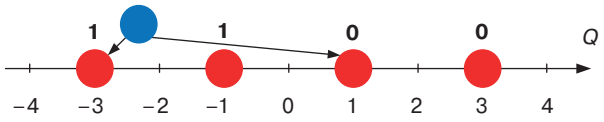

Fig. 6. Calculating the logarithm of the likelihood ratio for the 3rd bit

The logarithm of the likelihood ratio for b_2 of the received oscillation $\tilde{X}$ is the following:

$$l(b_2, \tilde{X}_i) \approx \frac{1}{2\sigma^2}((\Im(\tilde{X}_i)+3)^2 - (\Im(\tilde{X}_i)-1)^2) = \frac{2}{\sigma^2}(\Im(\tilde{X}_i)+1). \quad (11)$$

It follows from Fig. 3d that the value of b_3 affects the projection of the signal point on the *Q*-axis only. When $b_3 = 0$, this projection takes −3. When $b_3 = 1$, the projection takes −1, as shown in Fig. 7.

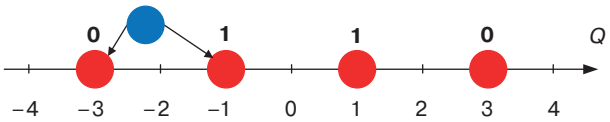

Fig. 7. Calculating the logarithm of the likelihood ratio for the 4th bit

The likelihood ratio for the fourth bit b_3 of the received oscillation $\tilde{X}$ is as follows:

$$l(b_3, \tilde{X}_i) \approx \frac{1}{2\sigma^2}((\Im(\tilde{X}_i)+1)^2 - (\Im(\tilde{X}_i)+3)^2) = -\frac{2}{\sigma^2}(\Im(\tilde{X}_i)+2). \quad (12)$$

Previously, the procedure of soft decision-making has been detailed on the basis of the specific example of the input oscillation depicted as a blue circle in Fig. 3. Similarly, after considering all possible positions of the input oscillation, the following is obtained:

$$l(b_0,\tilde{X}_i)=\begin{cases}-\frac{2}{\sigma^2}[\Re(\tilde{X}_i)+1], & \Re(\tilde{X}_i)<-2,\\ -\frac{2}{\sigma^2}\Re(\tilde{X}_i), & -2\le\Re(\tilde{X}_i)<0,\\ -\frac{2}{\sigma^2}\Re(\tilde{X}_i), & 0\le\Re(\tilde{X}_i)<2,\\ -\frac{2}{\sigma^2}[\Re(\tilde{X}_i)-1], & 2\le\Re(\tilde{X}_i),\end{cases} \quad (13)$$

$$l(b_1,\tilde{X}_i)=\frac{2}{\sigma^2}[|\Re(\tilde{X}_i)|-2] \quad \forall\Re(\tilde{X}_i), \quad (14)$$

$$l(b_2,\tilde{X}_i)=\begin{cases}\frac{2}{\sigma^2}[\Im(\tilde{X}_i)+1], & \Im(\tilde{X}_i)<-2,\\ \frac{2}{\sigma^2}\Im(\tilde{X}_i), & -2\le\Im(\tilde{X}_i)<0,\\ \frac{2}{\sigma^2}\Im(\tilde{X}_i), & 0\le\Im(\tilde{X}_i)<2,\\ \frac{2}{\sigma^2}[\Im(\tilde{X}_i)-1], & 2\le\Im(\tilde{X}_i),\end{cases} \quad (15)$$

$$l(b_3,\tilde{X}_i)=\frac{2}{\sigma^2}[|\Im(\tilde{X}_i)|-2] \quad \forall\Im(\tilde{X}_i). \quad (16)$$

The demodulation process for 64-QAM signals can be considered in a similar way to the soft decision-making for 16-QAM signal. The signal constellation, the received oscillation and signal points closest to it, corresponding to 0 and 1 for each of the six bits $b_0b_1b_2b_3b_4b_5$, contained in one symbol of 64-QAM signal are shown in Fig. 8, similar to Fig. 3.

Figure 8 shows that the first three bits affect the real part of the signal only, i.e., they determine the signal projection on the *I*-axis. The remaining three bits affect its imaginary part only, thus determining the projection on the *Q*-axis. According to these projections, the logarithms of likelihood ratios for all six bits can be unambiguously determined. The corresponding formulas are given in Tables 2 and 3.

For 256-QAM modulation, each point of this constellation corresponds to eight bits of the transmitted information: $b_0b_1b_2b_3b_4b_5b_6b_7$. A thorough examination of this constellation indicates that the first four bits affect the real part of the signal only, i.e., signal projections on the *I*-axis. The remaining four bits determine the imaginary part of the signal only, i.e., signal projections on the *Q*-axis. The calculation results for the logarithms of the likelihood ratios for all eight bits are summarized in Tables 4 and 5.

Table 2. Values of $l(b_k,\tilde{X}_i)$ for k = 0, 1, 2 for 64-QAM signal

$\Re(\tilde{X}_i)$	$l(b_0,\tilde{X}_i)$	$l(b_1,\tilde{X}_i)$	$l(b_2,\tilde{X}_i)$
$\Re(\tilde{X}_i)<-6$	$-8[\Re(\tilde{X}_i)+3]$	$-4[\Re(\tilde{X}_i)+5]$	$-2[\Re(\tilde{X}_i)+6]$
$-6\le\Re(\tilde{X}_i)<-4$	$-6[\Re(\tilde{X}_i)+2]$	$-2[\Re(\tilde{X}_i)+4]$	$-2[\Re(\tilde{X}_i)+6]$
$-4\le\Re(\tilde{X}_i)<-2$	$-4[\Re(\tilde{X}_i)+1]$	$-2[\Re(\tilde{X}_i)+4]$	$2[\Re(\tilde{X}_i)+2]$
$-2\le\Re(\tilde{X}_i)<0$	$-2\Re(\tilde{X}_i)$	$-4[\Re(\tilde{X}_i)+3]$	$2[\Re(\tilde{X}_i)+2]$
$0\le\Re(\tilde{X}_i)<2$	$-2\Re(\tilde{X}_i)$	$4[\Re(\tilde{X}_i)-3]$	$-2[\Re(\tilde{X}_i)-2]$
$2\le\Re(\tilde{X}_i)<4$	$-4[\Re(\tilde{X}_i)-1]$	$2[\Re(\tilde{X}_i)-4]$	$-2[\Re(\tilde{X}_i)-2]$
$4\le\Re(\tilde{X}_i)<6$	$-6[\Re(\tilde{X}_i)-2]$	$2[\Re(\tilde{X}_i)-4]$	$2[\Re(\tilde{X}_i)-6]$
$\Re(\tilde{X}_i)\ge6$	$-8[\Re(\tilde{X}_i)-3]$	$4[\Re(\tilde{X}_i)-5]$	$2[\Re(\tilde{X}_i)-6]$

Table 3. Values of $l(b_k,\tilde{X}_i)$ for k = 3, 4, 5 for 64-QAM signal

$\Im(\tilde{X}_i)$	$l(b_3,\tilde{X}_i)$	$l(b_4,\tilde{X}_i)$	$l(b_5,\tilde{X}_i)$
$\Im(\tilde{X}_i)<-6$	$8[\Im(\tilde{X}_i)+3]$	$-4[\Im(\tilde{X}_i)+5]$	$-2[\Im(\tilde{X}_i)+6]$
$-6\le\Im(\tilde{X}_i)<-4$	$6[\Im(\tilde{X}_i)+2]$	$-2[\Im(\tilde{X}_i)+4]$	$-2[\Im(\tilde{X}_i)+6]$
$-4\le\Im(\tilde{X}_i)<-2$	$4[\Im(\tilde{X}_i)+1]$	$-2[\Im(\tilde{X}_i)+4]$	$2[\Im(\tilde{X}_i)+2]$
$-2\le\Im(\tilde{X}_i)<0$	$2\Im(\tilde{X}_i)$	$-4[\Im(\tilde{X}_i)+3]$	$2[\Im(\tilde{X}_i)+2]$
$0\le\Im(\tilde{X}_i)<2$	$2\Im(\tilde{X}_i)$	$4[\Im(\tilde{X}_i)-3]$	$-2[\Im(\tilde{X}_i)-2]$
$2\le\Im(\tilde{X}_i)<4$	$4[\Im(\tilde{X}_i)-1]$	$2[\Im(\tilde{X}_i)-4]$	$-2[\Im(\tilde{X}_i)-2]$
$4\le\Im(\tilde{X}_i)<6$	$6[\Im(\tilde{X}_i)-2]$	$2[\Im(\tilde{X}_i)-4]$	$2[\Im(\tilde{X}_i)-6]$
$\Im(\tilde{X}_i)\ge6$	$8[\Im(\tilde{X}_i)-3]$	$4[\Im(\tilde{X}_i)-5]$	$2[\Im(\tilde{X}_i)-6]$

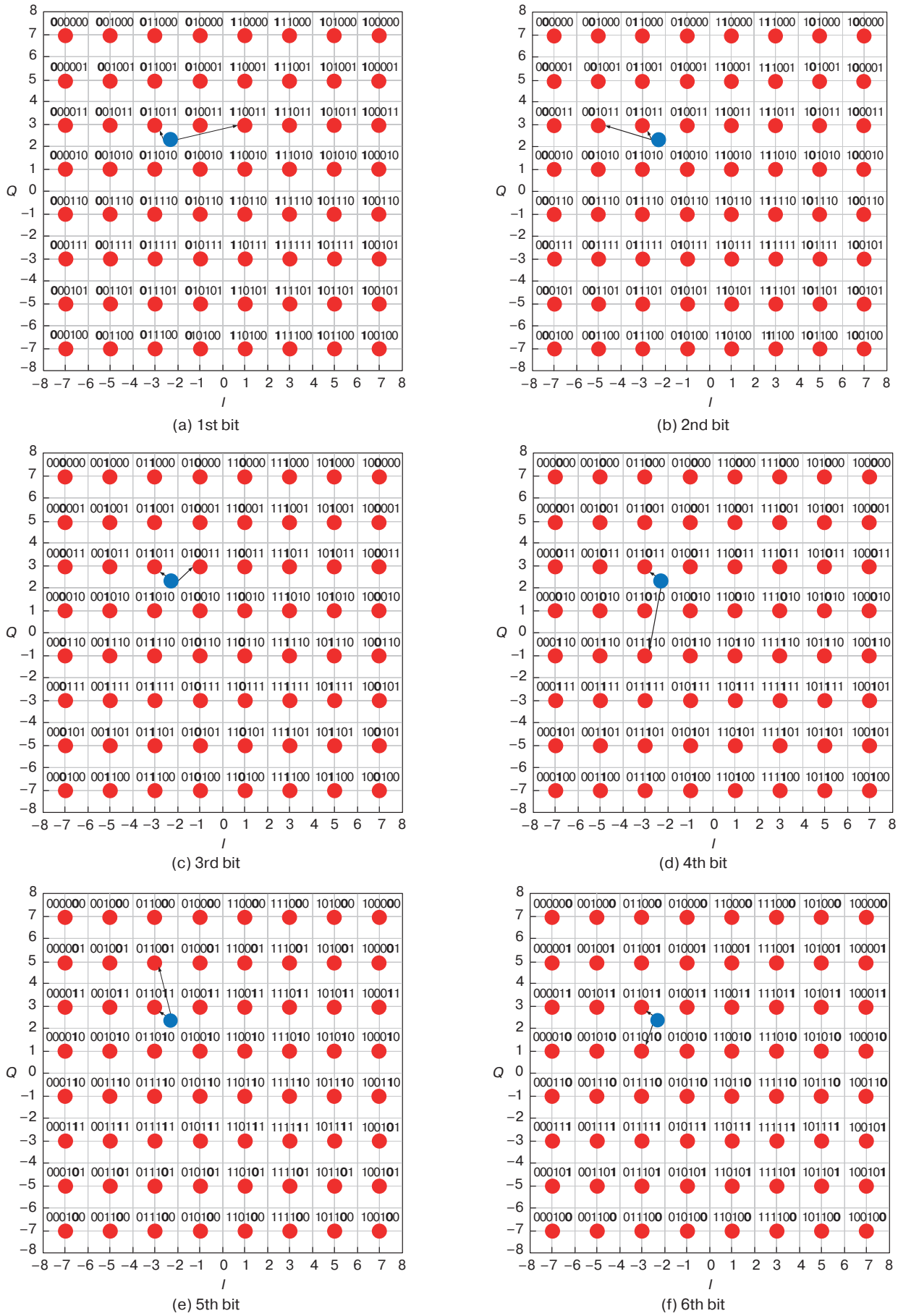

Fig. 8. Example of calculating the logarithms of likelihood ratios for each bit of the 64-QAM signal

Table 4. Values of $l(b_k,\tilde{X}_i)$ for k = 0, 1, 2, 3 for 256-QAM signal

$\Re(\tilde{X}_i)$	$l(b_0,\tilde{X}_i)$	$l(b_1,\tilde{X}_i)$	$l(b_2,\tilde{X}_i)$	$l(b_3,\tilde{X}_i)$
$\Re(\tilde{X}_i) \le -14$	$-16[\Re(\tilde{X}_i)+7]$	$-8[\Re(\tilde{X}_i)+11]$	$-4[\Re(\tilde{X}_i)+13]$	$-2[\Re(\tilde{X}_i)+14]$
$-14 \le \Re(\tilde{X}_i) < -12$	$-14[\Re(\tilde{X}_i)+6]$	$-6[\Re(\tilde{X}_i)+10]$	$-2[\Re(\tilde{X}_i)+12]$	$-2[\Re(\tilde{X}_i)+14]$
$-12 \le \Re(\tilde{X}_i) < -10$	$-12[\Re(\tilde{X}_i)+5]$	$-4[\Re(\tilde{X}_i)+9]$	$-2[\Re(\tilde{X}_i)+12]$	$2[\Re(\tilde{X}_i)+10]$
$-10 \le \Re(\tilde{X}_i) < -8$	$-10[\Re(\tilde{X}_i)+4]$	$-2[\Re(\tilde{X}_i)+8]$	$-4[\Re(\tilde{X}_i)+11]$	$2[\Re(\tilde{X}_i)+10]$
$-8 \le \Re(\tilde{X}_i) < -6$	$-8[\Re(\tilde{X}_i)+3]$	$-2[\Re(\tilde{X}_i)+8]$	$4[\Re(\tilde{X}_i)+5]$	$-2[\Re(\tilde{X}_i)+6]$
$-6 \le \Re(\tilde{X}_i) < -4$	$-6[\Re(\tilde{X}_i)+2]$	$-4[\Re(\tilde{X}_i)+7]$	$2[\Re(\tilde{X}_i)+4]$	$-2[\Re(\tilde{X}_i)+6]$
$-4 \le \Re(\tilde{X}_i) < -2$	$-4[\Re(\tilde{X}_i)+1]$	$-6[\Re(\tilde{X}_i)+6]$	$2[\Re(\tilde{X}_i)+4]$	$2[\Re(\tilde{X}_i)+2]$
$-2 \le \Re(\tilde{X}_i) < 0$	$-2\Re(\tilde{X}_i)$	$-8[\Re(\tilde{X}_i)+5]$	$4[\Re(\tilde{X}_i)+3]$	$2[\Re(\tilde{X}_i)+2]$
$0 \le \Re(\tilde{X}_i) < 2$	$-2\Re(\tilde{X}_i)$	$8[\Re(\tilde{X}_i)-5]$	$-4[\Re(\tilde{X}_i)-3]$	$-2[\Re(\tilde{X}_i)-2]$
$2 \le \Re(\tilde{X}_i) < 4$	$-4[\Re(\tilde{X}_i)-1]$	$6[\Re(\tilde{X}_i)-6]$	$-2[\Re(\tilde{X}_i)-4]$	$-2[\Re(\tilde{X}_i)-2]$
$4 \le \Re(\tilde{X}_i) < 6$	$-6[\Re(\tilde{X}_i)-2]$	$4[\Re(\tilde{X}_i)-7]$	$-2[\Re(\tilde{X}_i)-4]$	$2[\Re(\tilde{X}_i)-6]$
$6 \le \Re(\tilde{X}_i) < 8$	$-8[\Re(\tilde{X}_i)-3]$	$2[\Re(\tilde{X}_i)-8]$	$-4[\Re(\tilde{X}_i)-5]$	$2[\Re(\tilde{X}_i)-6]$
$8 \le \Re(\tilde{X}_i) < 10$	$-10[\Re(\tilde{X}_i)-4]$	$2[\Re(\tilde{X}_i)-8]$	$4[\Re(\tilde{X}_i)-11]$	$-2[\Re(\tilde{X}_i)-10]$
$10 \le \Re(\tilde{X}_i) < 12$	$-12[\Re(\tilde{X}_i)-5]$	$4[\Re(\tilde{X}_i)-9]$	$2[\Re(\tilde{X}_i)-12]$	$-2[\Re(\tilde{X}_i)-10]$
$12 \le \Re(\tilde{X}_i) < 14$	$-14[\Re(\tilde{X}_i)-6]$	$6[\Re(\tilde{X}_i)-10]$	$2[\Re(\tilde{X}_i)-12]$	$2[\Re(\tilde{X}_i)-14]$
$\Re(\tilde{X}_i) \ge 14$	$-16[\Re(\tilde{X}_i)-7]$	$8[\Re(\tilde{X}_i)-11]$	$4[\Re(\tilde{X}_i)-13]$	$2[\Re(\tilde{X}_i)-14]$

Table 5. Values of $l(b_k,\tilde{X}_i)$ for k = 4, 5, 6, 7 for 256-QAM signal

$\Im(\tilde{X}_i)$	$l(b_4,\tilde{X}_i)$	$l(b_5,\tilde{X}_i)$	$l(b_6,\tilde{X}_i)$	$l(b_7,\tilde{X}_i)$
$\Im(\tilde{X}_i) \le -14$	$16[\Im(\tilde{X}_i)+7]$	$-8[\Im(\tilde{X}_i)+11]$	$-4[\Im(\tilde{X}_i)+13]$	$-2[\Im(\tilde{X}_i)+14]$
$-14 \le \Im(\tilde{X}_i) < -12$	$14[\Im(\tilde{X}_i)+6]$	$-6[\Im(\tilde{X}_i)+10]$	$-2[\Im(\tilde{X}_i)+12]$	$-2[\Im(\tilde{X}_i)+14]$
$-12 \le \Im(\tilde{X}_i) < -10$	$12[\Im(\tilde{X}_i)+5]$	$-4[\Im(\tilde{X}_i)+9]$	$-2[\Im(\tilde{X}_i)+12]$	$2[\Im(\tilde{X}_i)+10]$
$-10 \le \Im(\tilde{X}_i) < -8$	$10[\Im(\tilde{X}_i)+4]$	$-2[\Im(\tilde{X}_i)+8]$	$-4[\Im(\tilde{X}_i)+11]$	$2[\Im(\tilde{X}_i)+10]$
$-8 \le \Im(\tilde{X}_i) < -6$	$8[\Im(\tilde{X}_i)+3]$	$-2[\Im(\tilde{X}_i)+8]$	$4[\Im(\tilde{X}_i)+5]$	$-2[\Im(\tilde{X}_i)+6]$
$-6 \le \Im(\tilde{X}_i) < -4$	$6[\Im(\tilde{X}_i)+2]$	$-4[\Im(\tilde{X}_i)+7]$	$2[\Im(\tilde{X}_i)+4]$	$-2[\Im(\tilde{X}_i)+6]$
$-4 \le \Im(\tilde{X}_i) < -2$	$4[\Im(\tilde{X}_i)+1]$	$-6[\Im(\tilde{X}_i)+6]$	$2[\Im(\tilde{X}_i)+4]$	$2[\Im(\tilde{X}_i)+2]$
$-2 \le \Im(\tilde{X}_i) < 0$	$2\Im(\tilde{X}_i)$	$-8[\Im(\tilde{X}_i)+5]$	$4[\Im(\tilde{X}_i)+3]$	$2[\Im(\tilde{X}_i)+2]$
$0 \le \Im(\tilde{X}_i) < 2$	$2\Im(\tilde{X}_i)$	$8[\Im(\tilde{X}_i)-5]$	$-4[\Im(\tilde{X}_i)-3]$	$-2[\Im(\tilde{X}_i)-2]$
$2 \le \Im(\tilde{X}_i) < 4$	$4[\Im(\tilde{X}_i)-1]$	$6[\Im(\tilde{X}_i)-6]$	$-2[\Im(\tilde{X}_i)-4]$	$-2[\Im(\tilde{X}_i)-2]$
$4 \le \Im(\tilde{X}_i) < 6$	$6[\Im(\tilde{X}_i)-2]$	$4[\Im(\tilde{X}_i)-7]$	$-2[\Im(\tilde{X}_i)-4]$	$2[\Im(\tilde{X}_i)-6]$
$6 \le \Im(\tilde{X}_i) < 8$	$8[\Im(\tilde{X}_i)-3]$	$2[\Im(\tilde{X}_i)-8]$	$-4[\Im(\tilde{X}_i)-5]$	$2[\Im(\tilde{X}_i)-6]$
$8 \le \Im(\tilde{X}_i) < 10$	$10[\Im(\tilde{X}_i)-4]$	$2[\Im(\tilde{X}_i)-8]$	$4[\Im(\tilde{X}_i)-11]$	$-2[\Im(\tilde{X}_i)-10]$
$10 \le \Im(\tilde{X}_i) < 12$	$12[\Im(\tilde{X}_i)-5]$	$4[\Im(\tilde{X}_i)-9]$	$2[\Im(\tilde{X}_i)-12]$	$-2[\Im(\tilde{X}_i)-10]$
$12 \le \Im(\tilde{X}_i) < 14$	$14[\Im(\tilde{X}_i)-6]$	$6[\Im(\tilde{X}_i)-10]$	$2[\Im(\tilde{X}_i)-12]$	$2[\Im(\tilde{X}_i)-14]$
$\Im(\tilde{X}_i) \ge 14$	$16[\Im(\tilde{X}_i)-7]$	$8[\Im(\tilde{X}_i)-11]$	$4[\Im(\tilde{X}_i)-13]$	$2[\Im(\tilde{X}_i)-14]$

Tables 2–5 show the equations required to calculate a small number of logarithms of likelihood ratios sufficient for a simplified decision-making algorithm for each of the bits defining any signal point of the QAM constellation. The equations are finalized in a form convenient for their practical use. The proposed algorithm requires significantly fewer calculations than the maximum likelihood algorithm which involves calculating logarithms of likelihood ratios for all possible combinations of bits.

The soft decision-making algorithm was developed for channels with white Gaussian noise. The efficiency of this algorithm for receiving OFDM signals in the presence of narrowband interference using soft decision encoding requires further analysis. These issues are discussed in the next section.

NOISE IMMUNITY OF QAM-OFDM SIGNAL RECEPTION

Below are the results of studying noise immunity when receiving QAM-OFDM signals in the presence of noise interference or a mixture of noise and narrowband interference. The study investigated the efficiency of using encoding to handle narrowband interference with demodulator soft decisions obtained using the algorithms described above.

The OFDM system was modeled using the *MATLAB*[1] tool. The number of FFT points in the formation of the OFDM signal amounts to 128, the guard interval length is –32, and the methods for modulating subcarriers are 16-QAM, 64-QAM, and 256-QAM.

The focus of the study was on modeling the signal and interference. According to Fig. 2, complex envelopes of signals are represented by numbers $(a + jb)$, where $a,b \in \{\pm1,\pm3,...,\pm(\sqrt{M}-1)\}$. In this case, the average signal strength is dependent on modulation multiplicity M. For comparable simulation results at different modulation multiplicities, coefficient l depending on M need to be introduced into the signal representation. Then complex envelopes of signals may be represented by numbers, as follows:

$$l(a+jb), \text{ where } a,b \in \{\pm1,\pm3,...,\pm(\sqrt{M}-1)\}.$$

Coefficient l should be selected so that the signal energy per transmitted symbol E_s does not depend on modulation multiplicity M. The average energy of a single symbol of M-QAM signal with duration T_s is as follows:

$$E_s = \frac{T_s}{M}\sum_{i=1}^{M}\frac{l^2(a_i^2+b_i^2)}{2}.$$

For certainty, $E_s = 1$ and $T_s = 1$ are assumed in modeling, while the desired signal-to-noise ratio (SNR) is provided by selecting the noise variance. Then

$$1 = \frac{l^2}{M}\sum_{i=1}^{M}\frac{(a_i^2+b_i^2)}{2}.$$

According to this relationship, it follows that $l = \frac{1}{\sqrt{5}}$ for 16-QAM signal, $l = \frac{1}{\sqrt{21}}$ for 64-QAM signal, and $l = \frac{1}{\sqrt{85}}$ for 256-QAM signal.

The energy per bit of the transmitted information is as follows:

$$E_b = E_s / \log_2 M = \frac{1}{\log_2 M}.$$

In the OFDM system, subcarriers are located on the frequency axis at distance $\frac{1}{T_s}$ apart. The noise variance in this band is $\sigma_n^2 = \frac{N_0}{T_s} = N_0$ (N_0 is single-sided noise spectral density).

The SNR, understood as the ratio of the average signal energy per bit of transmitted information to the noise spectral density:

$$\frac{E_b}{N_0} = \frac{1}{\sigma_n^2 \log_2 M}.$$

Hence, it may be written in the following way:

$$\sigma_n^2 = \frac{1}{\frac{E_b}{N_0}\log_2 M}.$$

This means that since the signal energy is assumed equal to one for all types of M-QAM modulation, the Gaussian noise with variance $\sigma_n^2 = \frac{1}{\frac{E_b}{N_0}\log_2 M}$ should be modeled to obtain the desired SNR $\frac{E_b}{N_0}$.

Figures 9–11 show the dependencies of bit error rate (BER) P_{eb} on SNR per bit of transmitted information for 16-QAM, 64-QAM, and 256-QAM. The simulation is performed for a channel with white Gaussian noise in the absence and in the presence of narrowband interference for the signal to interference ratio (SIR) equal to 0 dB in power. The transmission methods without encoding,

[1] https://www.mathworks.com/products/matlab.html. Accessed March 31, 2024.

with low-density parity-check (LDPC) encoding [19], and with convolutional encoding under soft and hard demodulator decisions were investigated. The code rate (R) is 1/2 for all types of encoding.

The convolutional code considered in this case is based on generating polynomials $G_1(X) = 1 + X + X^2 + X^3 + X^4$ and $G_2(X) = 1 + X + X^3 + X^4$. This code is decoded using the Viterbi algorithm. Using the convolutional code at rate 3/4 is also discussed below. The code is obtained from the code at rate 1/2 by poking every third output bit according to the pattern $\begin{bmatrix} 1 & 1 & 0 \\ 1 & 0 & 1 \end{bmatrix}$.

At LDPC encoding at rate 1/2, the codeword length totals 648 bits, 324 of them being information ones. Soft decoding was performed according to the Belief propagation algorithm (or sum of products).

It can be seen in each figure that when encoding is used, BER P_{eb} is significantly reduced when compared to cases without encoding.

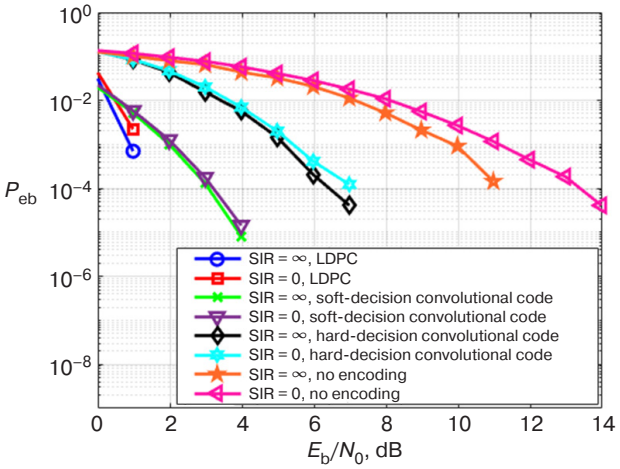

Fig. 9. Dependence of BER P_{eb} on SNR E_b/N_0 for OFDM system with 16-QAM modulation and different types of encoding

Figure 9 shows that in the presence of narrowband interference and for $P_{eb} = 10^{-3}$, LDPC encoding gives 10 dB better results than no encoding, 4 dB better results than in the case of convolutional encoding with hard decision, and 1 dB better results than convolutional encoding with soft decision.

It follows from Fig. 10 that in the presence of narrowband interference and for $P_{eb} = 10^{-3}$, LDPC encoding gives 16 dB better results than no encoding, 6 dB better results than in the case of convolutional encoding with hard decision, and 1.5 dB better results than convolutional encoding with soft decision.

Figure 11 shows that in the presence of narrowband interference and at $P_{eb} = 10^{-3}$, LDPC encoding gives 10 dB better result than convolutional encoding with hard decision, and 2 dB better result than in the case of convolutional encoding with soft decision.

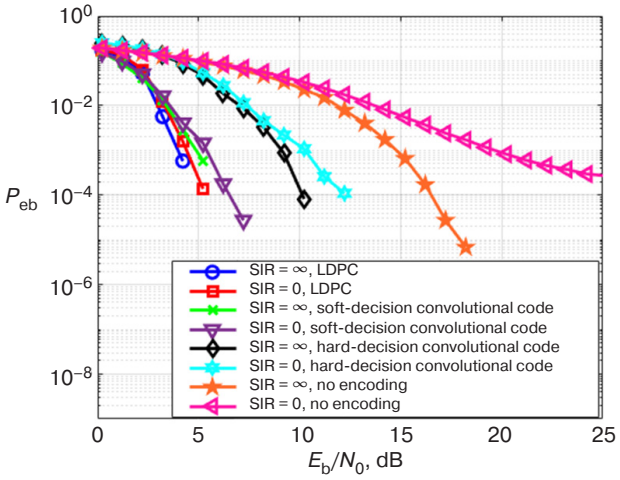

Fig. 10. Dependence of BER P_{eb} on SNR E_b/N_0 for OFDM system with 64-QAM modulation and different types of encoding

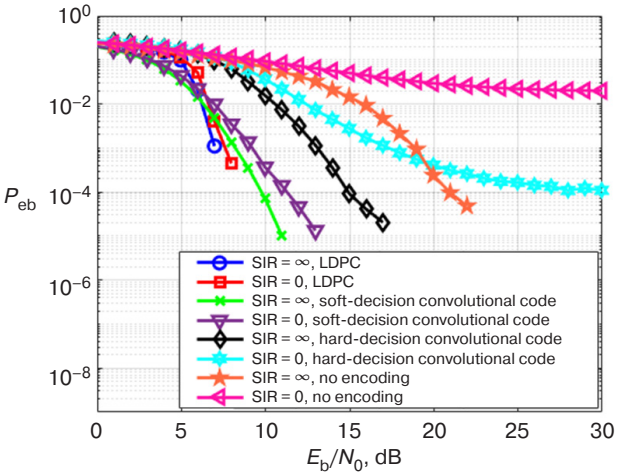

Fig. 11. Dependence of BER P_{eb} on SNR E_b/N_0 for OFDM system with 256-QAM modulation and different types of encoding

Figures 9–11 suggests that in the presence of narrowband interference, the encoding reduces BER significantly compared to the case of no encoding. Encoding with soft demodulator decisions gives better results than with hard decisions. LDPC encoding with soft decisions gives better results than in the case of convolutional encoding with soft decisions.

Figures 12–14 show simulation results comparing the efficiencies of convolutional encoding and LDPC encoding with soft demodulator decisions and with $R = 1/2$ and 3/4 in the presence of narrowband interference: SIR is 0 dB in power.

It can be seen from Fig. 12 that at $P_{eb} = 10^{-3}$, LDPC encoding with soft demodulator decisions at $R = 1/2$ is 3.5 dB better than at $R = 3/4$. Convolutional encoding with soft demodulator decisions at $R = 1/2$ is 5 dB better than at $R = 3/4$. When $R = 1/2$, LDPC encoding with soft demodulator decisions is 0.5 dB better than in the case of convolutional encoding with soft demodulator decisions.

When R = 3/4, LDPC encoding with soft demodulator decisions is 5 dB better than in the case of convolutional encoding with soft demodulator decisions.

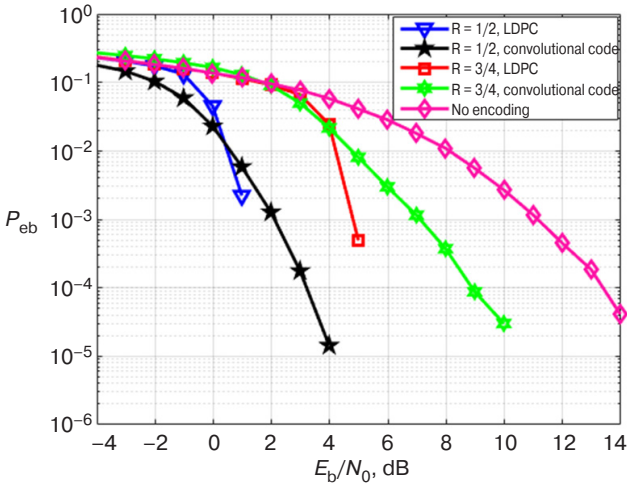

Fig. 12. Dependence of BER P_{eb} on SNR E_b/N_0 for OFDM system with 16-QAM modulation and different code rates

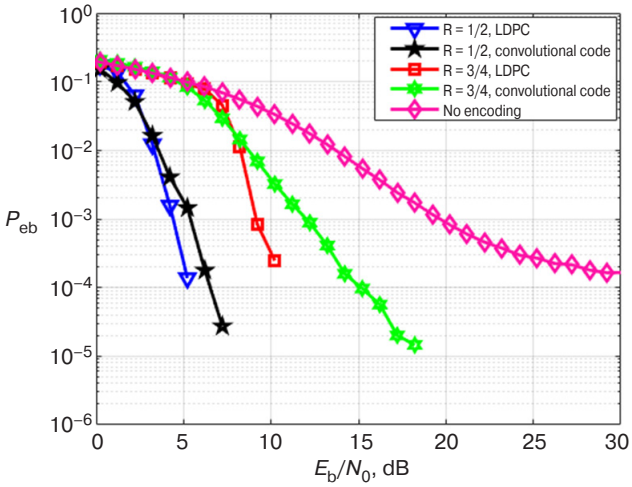

Fig. 13. Dependence of BER P_{eb} on SNR E_b/N_0 for OFDM system with 64-QAM modulation and different code rates

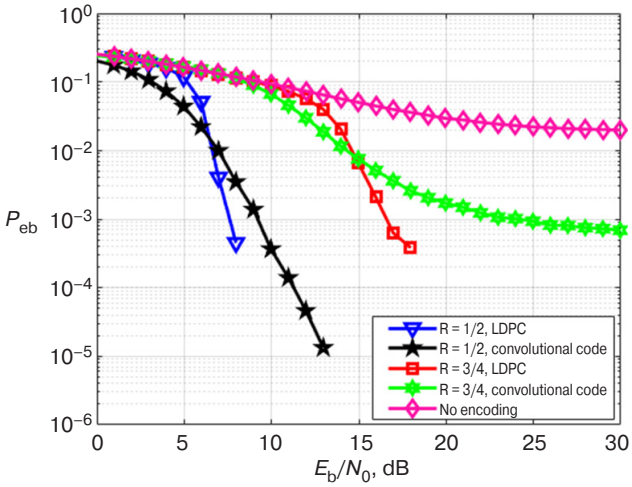

Fig. 14. Dependence of BER P_{eb} on SNR E_b/N_0 for OFDM system with 256-QAM modulation and different code rates

Figure 13 shows that at $P_{eb} = 10^{-3}$, LDPC encoding with soft demodulator decisions at R = 1/2 is energetically 4.5 dB better than at R = 3/4. The convolutional encoding with soft demodulator decisions at R = 1/2 is 6.5 dB better than at R = 3/4. At R = 1/2, LDPC encoding with soft demodulator decisions is 1 dB better than in the case of convolutional encoding with soft demodulator decisions. At R = 3/4, LDPC encoding with soft demodulator decisions is 3 dB better than convolutional encoding with soft demodulator decisions.

Figure 14 shows that at $P_{eb} = 10^{-3}$, LDPC encoding with soft demodulator decisions at R = 1/2 is 9 dB better than at R = 3/4. The convolutional encoding with soft demodulator decisions at R = 1/2 is 14 dB better than at R = 3/4. At R = 1/2, LDPC encoding with soft demodulator decisions is 1.5 dB better than convolutional encoding with soft demodulator decisions. At R = 3/4, LDPC encoding with soft demodulator decisions is 6.5 dB better than in the case of convolutional encoding with soft demodulator decisions.

Figures 12–14 suggest that LDPC encoding gives better results than convolutional encoding with soft demodulator decisions. In this case, R = 1/2 produces better reception immunity than rate 3/4.

Figures 15–17 show the results of evaluating the reception immunity of OFDM signal with QAM subcarrier modulation using soft demodulator decisions at SIR values: R = 1/2 for all types of encoding.

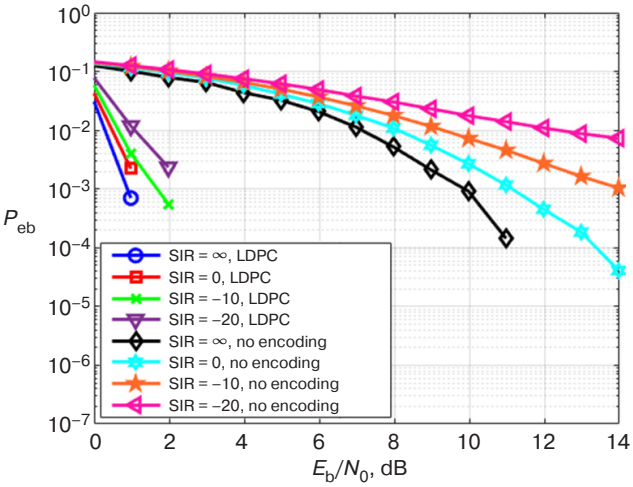

Fig. 15. Dependence of BER on SNR E_b/N_0 for OFDM system with 16-QAM in the presence of narrowband interference with different levels

Figure 15 shows that at $P_{eb} = 10^{-3}$, when there is no narrowband interference (SIR = ∞), LDPC encoding gives 9 dB better results than when no encoding is used. At SIR = 0 dB, LDPC encoding gives 10 dB better results than no encoding. At SIR = −10 dB,

LDPC encoding gives 11 dB better results than no encoding. At $P_{eb} = 10^{-3}$, when SIR = −20 dB, LDPC encoding gives at least 20 dB better results than transmission without encoding.

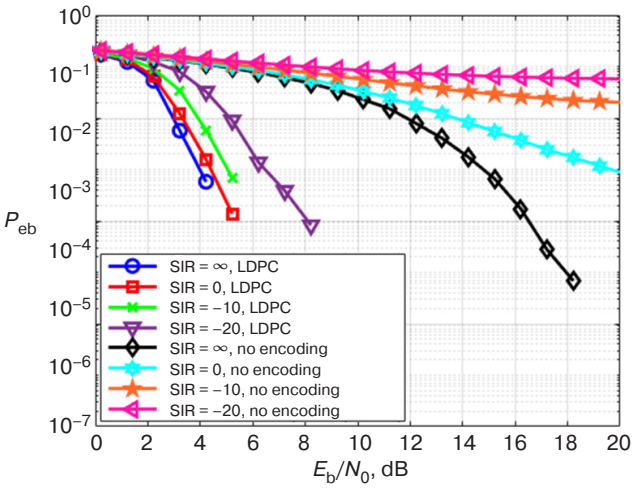

Fig. 16. Dependence of BER on SNR E_b/N_0 for OFDM system with 64-QAM in the presence of narrowband interference with different levels

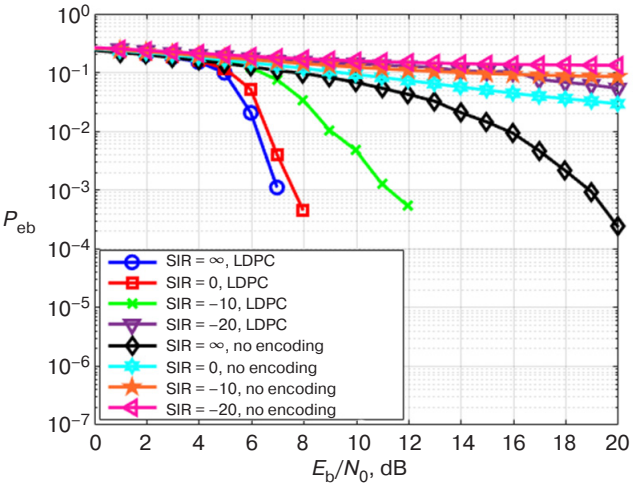

Fig. 17. Dependence of BER on SNR E_b/N_0 for OFDM system with 256-QAM in the presence of narrowband interference with different levels

Figure 16 shows that at $P_{eb} = 10^{-3}$, when there is no narrowband interference (SIR = ∞), LDPC encoding gives 11 dB better results than no encoding. At SIR = 0 dB, LDPC encoding gives 15.5 dB better results than no encoding. At SIR = –10 dB, BER drops below 10^{-3} with E_b/N_0 higher than 5 dB. At SIR = –20 dB. This occurs at E_b/N_0 higher than 8 dB.

Figure 17 shows that at $P_{eb} = 10^{-3}$, when there is no narrowband interference (SIR = ∞), LDPC encoding gives 12 dB better results than no encoding. At SIR = 0 dB, BER drops lower than 10^{-3} when E_b/N_0 is greater than 8 dB. At SIR = –10 dB, BER drops lower than 10^{-3} when E_b/N_0 is higher than 12 dB.

The results shown in Figs. 15–17 describe the noise immunity of OFDM signal reception in the presence of narrowband interference at different SIR with and without LDPC encoding. It can be observed that for all three types of modulation, the narrowband interference significantly degrades the noise immunity of the transmission system in the absence of encoding, and the noise immunity drops more significantly with increasing QAM multiplicity. The LDPC code reduces the impact of narrowband interference on the system significantly, being especially noticeable at small QAM multiplicities.

CONCLUSIONS

Based on these findings, it can be concluded that the use of encoding with soft demodulator decisions significantly improves the noise immunity of OFDM signal reception, while mitigating the impact of narrowband interference on the transmission system. LDPC encoding is superior to convolutional encoding in improving the noise immunity of OFDM signal reception, including in the presence of narrowband interference. In addition to use in QAM-OFDM systems, the proposed simple demodulation method for soft decision QAM signals can be applied to any wireless communication system using M-QAM signals, where M is number 2 to an even power.

Authors' contributions. All authors equally contributed to the research work.

REFERENCES

1. Cimini Jr. L.J. Analysis and simulation of a digital mobile channel using orthogonal frequency division multiplexing. *IEEE Trans. Commun*. 1985;33(7):665–675. Available from URL: https://doi.org/10.1109/TCOM.1985.1096357
2. Mosse P.H. A technique for orthogonal frequency division multiplexing frequency offset correction. *IEEE Trans. Commun*. 1994;42(10):2908–2914. https://doi.org/10.1109/26.328961
3. Van Nee R., Prasad R. *OFDM for Wireless Multimedia Communications*. Boston: Artech House; 2000. 260 p.
4. Pandey S., Bharti M., Agrawal A.K. Analysis of M-ary QAM-Based OFDM Systems in AWGN Channel. In: Bansal R.C., Agrawal A., Jadoun V.K. (Eds.). *Advances in Energy Technology: Select Proceedings of EMSME.* 2022;(766):223–235. https://doi.org/10.1007/978-981-16-1476-7_22
5. Van Wyk J., Linde L. Bit error probability for a M-ary QAM OFDM-based system. In: *AFRICON 2007*. IEEE; 2007. https://doi.org/10.1109/AFRCON.2007.4401578
6. Fuqin Xiong. M-ary amplitude shift keying OFDM system. *IEEE Trans. Commun*. 2003;51(10):1638–1642. https://doi.org/10.1109/TCOMM.2003.818103
7. Batra A., Zeidler J.R. Narrowband interference mitigation in OFDM systems. In: *MILCOM 2008. 2008 IEEE Military Communications Conference.* 2008. https://doi.org/10.1109/MILCOM.2008.4753296
8. Coleri S., Ergen M., Puri A., Bahai A. Channel estimation techniques based on pilot arrangement in OFDM systems. *IEEE Trans. Broadcast*. 2002;48(3):223–229. http://doi.org/10.1109/TBC.2002.804034
9. Lu B., Yue G., Wang X.D. Performance analysis and design optimization of LDPC-coded MIMO OFDM systems. *IEEE Trans. Signal Process.* 2004;52(2):348–361. https://doi.org/10.1109/TSP.2003.820991
10. Lu B., Wang X. Space-time code design in OFDM systems. In: *Globecom '00 – IEEE. Global Telecommunications Conference. Conference Record* (*Cat. No.00CH37137*). IEEE; 2000. V. 2. P. 1000–1004. https://doi.org/10.1109/GLOCOM.2000.891288
11. Wang Q., Onotera L.Y. Coded QAM using a binary convolutional code. *IEEE Trans. Commun.* 1995;43(6):2001–2004. https://doi.org/10.1109/26.387437
12. Mosleh M.F. Log-Likelihood Ratio to Improve Hard Decision Viterbi Algorithm. *Eng. & Tech. J.* 2013;31(9):1779–1790. https://doi.org/10.30684/etj.2013.82189
13. Hagenauer J., Hoeher P. A Viterbi algorithm with soft-decision outputs and its applications. In: *1989 IEEE Global Telecommunications Conference and Exhibition "Communications Technology for the 1990s and Beyond*." 1989;3:1680–1686. https://doi.org/10.1109/GLOCOM.1989.64230
14. Cao S., Kam P.Y., Yu C. Pilot-Aided Log-Likelihood Ratio for LDPC Coded MPSK-OFDM Transmission. *IEEE Photon. Technol. Lett.* 2013;25(6):594–597. https://doi.org/10.1109/LPT.2013.2246563
15. Cao S., Kam P.Y., Yu C. Pilot-aided log-likelihood ratio for LDPC coded M-QAM CO-OFDM system. *OFC 2014.* 2014, W3. https://doi.org/10.1364/OFC.2014.W3J.1
16. Chen J., Dholakia A., Ftheriou E., et al. Reduced-complexity decoding of LDPC codes. *IEEE Trans. Commun*. 2005;53(8):1288–1299. https://doi.org/10.1109/TCOMM.2005.852852
17. Jiabin T., Yue X., Lilin D., Wei X., et al. Efficient LLR Approximation for Coded Constant Envelope OFDM. *IEEE Trans. Vehicular Technol.* 2023;72(5):6194–6208. https://doi.org/10.1109/TVT.2022.3231912
18. Zhenyu Z., Caihong G., Hua L., et al. Soft-Input Soft-Output Detection via Expectation Propagation for Massive Spatial Modulation MIMO Systems. *IEEE Commun. Lett.* 2021;25(4):1173–1177. https://doi.org/10.1109/LCOMM.2020.3047081
19. Chu V.V. Noise immunity of OFDM transmission system when using LDPC code. In: *Fundamental, Exploratory, Applied Research and Innovation Projects: Proceedings of the National Scientific and Practical Conference*. Moscow: RTU MIREA; 2022. P. 389–392 (in Russ.).

About the authors

Alexey A. Paramonov, Dr. Sci. (Eng.), Professor, Department of Radio Electronic Systems and Complexes, Institute of Radio Electronics and Informatics, MIREA – Russian Technological University (78, Vernadskogo pr., Moscow, 119454 Russia). E-mail: paramonov@mirea.ru. Scopus Author ID 57208923552, RSCI SPIN-code 5605-9459, http://orcid.org/0000-0002-4537-4626

Chu Van Vuong, Postgraduate Student, Department of Radio Electronic Systems and Complexes, Institute of Radio Electronics and Informatics, MIREA – Russian Technological University (78, Vernadskogo pr., Moscow, 119454 Russia). E-mail: muadem1110@gmail.com. http://orcid.org/0009-0003-0143-0168

Об авторах

Парамонов Алексей Анатольевич, д.т.н., профессор, кафедра радиоэлектронных систем и комплексов, Институт радиоэлектроники и информатики, ФГБОУ ВО «МИРЭА – Российский технологический университет» (119454, Россия, Москва, пр-т Вернадского, д. 78). E-mail: paramonov@mirea.ru. Scopus Author ID 57208923552, SPIN-код РИНЦ 5605-9459, http://orcid.org/0000-0002-4537-4626

Чу Ван Вуонг, аспирант, кафедра радиоэлектронных систем и комплексов, Институт радиоэлектроники и информатики, ФГБОУ ВО «МИРЭА – Российский технологический университет» (119454, Россия, Москва, пр-т Вернадского, д. 78). E-mail: muadem1110@gmail.com. http://orcid.org/0009-0003-0143-0168

Translated from Russian into English by K. Nazarov
Edited for English language and spelling by Dr. David Mossop